

# How Does Pin1 Catalyze the Cis–Trans Prolyl Peptide Bond Isomerization? A QM/MM and Mean Reaction Force Study

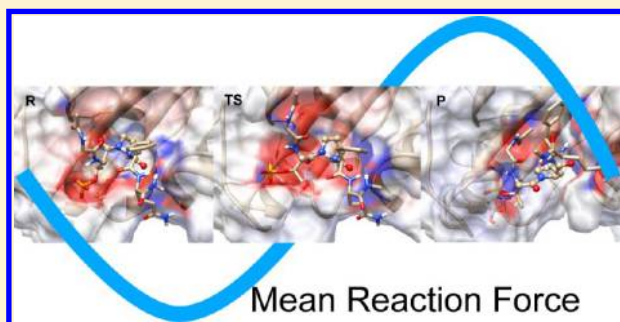
Esteban Vöhringer-Martinez,<sup>\*,†</sup> Fernanda Duarte,<sup>‡</sup> and Alejandro Toro-Labbé<sup>‡</sup>

<sup>†</sup>Departamento de Físico-Química, Facultad de Ciencias Químicas, Universidad de Concepción, Chile

<sup>‡</sup>Laboratorio de Química Teórica Computacional (QTC), Facultad de Química, Pontificia Universidad Católica de Chile, Santiago, Chile

**S** Supporting Information

**ABSTRACT:** Pin1 represents an enzyme that specifically catalyzes the isomerization of peptide bonds between phosphorylated threonine or serine residues and proline. Despite its relevance as molecular timer in a number of biological processes related to cancer and Alzheimer disease, a detailed understanding of the factors contributing to the catalysis is still missing. In this study, we employ extensive QM/MM molecular dynamics simulations in combination with the mean reaction force (MRF) to discern the influence of the enzyme on the reaction mechanism and the origin of the catalysis. As a recently introduced method, the MRF separates the activation free energy barrier to reach the transition state into structural and electronic contributions providing a more detailed description of the enzyme's function. As a reference, we first study the isomerization starting from the cis form in solution and obtain a free energy barrier and a reaction free energy, which are in agreement with previous studies and experiment. With the new mean reaction force method, intramolecular hydrogen bonds in the peptide were identified that stabilize the transition state and reduce the electronic contribution to the free energy barrier. To elucidate the mechanism of catalysis of Pin1, the reaction in solution and in the catalytic cavity of the enzyme were compared. Both yield the same free energy barrier for the isomerization of the cis form, but with different decomposition in structural and electronic contributions by the mean reaction force. The enzyme reduces the energy required for structural rearrangements to reach the transition state, pointing to a destabilization of the reactant, but increases the electronic contribution to the barrier through specific enzyme–peptide hydrogen bonds. In the reverse reaction, the isomerization of the trans form, the enzyme alters the energetics and the mechanism of the reaction considerably. Unfavorable enzyme–peptide interactions in the catalytic cavity during the isomerization change the reaction coordinate, resulting in two minima with small energy differences to the transition state. These small free energy barriers should in principle make the reaction feasible at room temperature once the conformer is bound in the right conformation.



## INTRODUCTION

In proteins, the peptide bonds between the amide nitrogen and the carbonyl carbon atom are typically found in the trans configuration. A special case is the peptide bond preceding a proline residue, where the cis conformation becomes feasible due to a steric interaction between the C $\delta$ -atom of the proline side chain and backbone atoms destabilizing the trans conformer.<sup>1,2</sup> The cis–trans isomerization of this peptide bond is a rather slow process at room temperature due to the large energy barrier, but has been shown to play an important role in protein folding.<sup>3,4</sup> This is likely because native proteins bear the cis isomer, which is not naturally synthesized in the ribosome. Additionally, the isomerization reaction is also used as a molecular timer in a number of biological processes, including cell signaling,<sup>5</sup> ion channel gating,<sup>6</sup> and gene expression,<sup>7,8</sup> and its deregulation is related to pathological conditions, such as cancer<sup>9,10</sup> and Alzheimer's disease.<sup>11,12</sup> Side-chain phosphorylation at threonine or serine residues preceding

the proline residue (pThr/pSer-Pro moieties) decelerates both cis to trans and trans to cis isomerization rates.<sup>13,14</sup> The conformers of these motifs have been shown to be critical and regulatory for many proteins, including kinases and phosphatases. In fact, a strict control of the cis/trans populations of these pThr/pSer-Pro motifs is needed to ensure proper regulation of cellular signaling.<sup>15</sup> In this context, the peptidyl-prolyl isomerase Pin1 has emerged as a critical regulator.<sup>16</sup> Pin1 specifically catalyzes the cis–trans isomerization of the pThr/pSer-Pro imide linkages with a selectivity over nonphosphorylated motifs of more than 1300-fold.<sup>17</sup>

Pin1 is a two domain-enzyme with a WW domain, which binds pThr/pSer-Pro motifs with high affinity, and a catalytic active peptidyl-prolyl isomerase (PPIase) domain. Studies have

**Received:** August 9, 2012

**Revised:** September 21, 2012

**Published:** October 2, 2012

shown that the catalytic PPIase domain possesses full isomerase activity even without the other domain and the flexible linker connecting the two.<sup>18</sup> At the entrance to the active site of the PPIase domain, a positively charged cluster formed by a triad of basic residues, Lys-63, Arg-68, and Arg-69, stabilizes the negative charged phosphate group of the pThr-Pro motif (see representative structure of equilibrated peptide Ace-Gly-pThr-Pro-Phe-Gln-Nme in Pin1 in Figure 1). The aliphatic proline

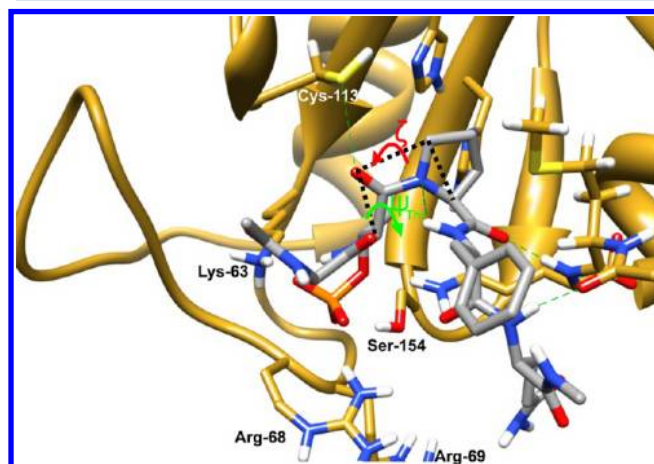


**Figure 1.** Snapshot of the catalytic active site of human Pin1 with the Ace-Gly-pThr-Pro-Phe-Gln-Nme peptide and the dihedral angle  $\zeta$  representing the reaction coordinate together with the  $\psi_{\text{Thr}}$  backbone angle, which also rotates in the activation of the trans form.

side chain is cradled in a hydrophobic pocket formed by the residues Phe-134, Met-130, and Leu-122. A hydrogen bond between the proline carbonyl oxygen atom and the backbone amide group of Gln-131 in the enzyme maintains this residue essentially fixed. Following the peptide sequence, a second hydrogen bond between the amide group of the glutamine residue and the carbonyl oxygen atom of the Gln-129 residue of the PPIase domain fixes this part of the peptide, inhibiting its rotation during the isomerization process (see Figure 1).

Although several experimental studies on PIN1 activity have been reported, the exact mechanism by which Pin1 catalyzes the cis–trans isomerization process remains elusive and is still a subject of controversy. Both covalent<sup>19,20</sup> and noncovalent<sup>21</sup> mechanisms have been invoked. According to the covalent mechanism, based on the original paper describing the crystal structure of Pin1, catalysis takes place first through a proton transfer process from the thiol group of Cys-113 to His-59, followed by a nucleophilic attack of the sulfur atom of Cys-113 to the carbonyl group. However, the fact that Cys113D and His59L mutants remain functional called this mechanism into question.<sup>21,22</sup> The noncovalent catalysis mechanism, on the other hand, suggests that Cys-113 plays a key role in maintaining an overall electronegative environment, which might destabilize the double bond character of the prolyl bond.<sup>21</sup> Experimental determination of the  $pK_a$  value of this residue, however, has not been possible so far to the best of our knowledge. To test the hypothesis of a negatively charged sulfur atom at this position contributing to the catalysis, we also studied a system where the proton of Cys-113 is transferred through His-59 to His-157 employing molecular dynamics simulations. During the course of the simulation, however, the peptide started moving out of the cavity. This observation together with the mutation studies showing no functional

dependence of the enzyme on His-59 and His-157<sup>21,22</sup> favors a neutral protonation state of Cys-113 during the isomerization reaction.

To discern the mechanism by which Pin1 catalyzes the isomerization, we studied the reaction in aqueous solution and compared it to the results obtained in the enzyme. Therefore, extensive QM/MM molecular dynamics simulations have been carried out for the reaction in the two different environments.

## METHODS

Molecular dynamics simulations were performed with the Gromacs 4.5.3 software package.<sup>23</sup> A time step of 2 fs in combination with the velocity rescaling temperature coupling algorithm of Bussi et al.<sup>24</sup> ( $\tau = 0.1$  ps) and the Berendsen pressure coupling algorithm<sup>25</sup> was used. The electrostatic interactions were calculated with the Particle Mesh-Ewald method, a cutoff radius of 1.0 nm, pme-order of 4, and a spacing of 0.1 nm. The van der Waals interactions were described by a shifting function, which switches the forces to zero between 0.8 and 0.9 nm. The neighbor list was updated every 5 steps, and its cutoff was set to 1.0 nm. All hydrogen bonds were constrained with the LINCS algorithm of order 4.<sup>26</sup>

The QM/MM molecular dynamics simulation was performed in combination with the Gaussian 03 package<sup>27</sup> in an electrostatic embedding as incorporated in the Gromacs 4.5.3 package. Electrostatic interactions in the MM region were treated with the reaction field method (cutoff radius = 1.0 nm, switching radius = 0.9 nm,  $\epsilon_r = 78$ ), and the time step was reduced to 1 fs. The neighbor list was updated at every step.

**System Setup.** The crystal structure of an inhibitor bound complex of Pin1 with PDB ID 2Q5A (1.5 Å resolution)<sup>28</sup> was used as a starting structure for this study. The inhibitor was modified to match the sequence of the substrate, Ace-Gly-pThr-Pro-Phe-Gln-Nme. Because the inhibitor already provided the substrate backbone, only redundant atoms were deleted, and the capping residues were added at the end positions. The AMBER99sb<sup>29</sup> force field was used in combination with the charges provided by Craft et al.<sup>30</sup> for the threonine phosphate group.

Residues 39–50 were not resolved in the crystal structure, which originates from their high flexibility as shown in various NMR studies.<sup>31,32</sup> To resolve this issue, a terminal group was added to the end residues Ser-38 and Glu-51. Additionally, a harmonic restraint ( $k = 400$  kJ mol<sup>−1</sup> nm<sup>−2</sup>, distance = 1.48 nm) was applied in all reported simulations on their  $C_\alpha$  atoms to maintain their interaction imposed by the missing residues. In a second step, this imposed restraint on the protein dynamics was validated modeling the missing residues with the Amber10 package and the xleap program: comparison of the two output structures with the unrestrained and restraint systems after an equilibration of 50 ns yielded no differences in the secondary structure nor in the catalytic cavity.

The obtained enzyme structure with the peptide substrate was solvated in a cubic box with a side length of 8 nm employing the SPC model for the water molecules.<sup>33</sup> Counter ions were added to obtain a physiological salt concentration (0.154 mol/L) of the neutral system. The whole simulation system was first minimized, simulated with position restraint on all  $C_\alpha$  atoms for 500 ps, and equilibrated for 50 ns.

The equilibrated structure, which contained the peptide bond in cis configuration, served as the starting structure for the isomerization to the trans isomer. The dihedral angle  $\zeta$ , defined by the atoms  $C_\alpha(\text{pThr})\text{--O}_{\text{CO}}(\text{pThr})\text{--}C_\delta(\text{Pro})\text{--}C_\alpha(\text{Pro})$  (see

Figure 1), was used as the reaction coordinate as proposed by Karplus et al.<sup>34,35</sup> The dihedral angle was restrained with a force constant of 500 kJ mol<sup>-1</sup> rad<sup>-2</sup> starting at 0° for 5 ns. The obtained output structure served as input for the subsequent 5 ns simulation where the dihedral angle was increased (anticlockwise) or decreased (clockwise) by 10°. This procedure was performed until 180°, which corresponds to the trans configuration. The subsequent use of output structures and the 5 ns equilibration ensures a proper equilibration of the peptide and the enzyme during the rotation.

In accordance with the results of Velazquez et al.,<sup>36</sup> a second reaction coordinate, described by the  $\psi_{\text{Thr}}$  angle of the threonine phosphate residue (see Figure 1), was introduced once 140° was reached. The second reaction coordinate was needed to avoid unfavorable interactions with the enzyme. The simulation procedure was the same, and  $\zeta$  and  $\psi_{\text{Thr}}$  values were chosen to match the minimum free energy path in Velazquez et al.'s<sup>36</sup> work: 140/90, 150/70, 160/50, 160/30, 160/10, 160/-10, 160/-30, 170/-30, 180/-30, and 180/-50.

The cis–trans isomerization was also performed in aqueous solution to identify the origin of the catalysis. For the aqueous solution simulations, the equilibrated peptide from the enzyme in the cis configuration was isolated and solvated in a cubic box with 5 nm box length and physiological NaCl concentration and equilibrated for 5 ns. The isomerization was performed in the same consecutive manner as described above along  $\zeta$ .

**QM/MM Molecular Dynamics.** Starting structures for the QM/MM simulations were obtained from the last 4 ns of the MM simulations along the reaction path. The QM region involved all atoms in the amino acid sequence starting at the C $_{\alpha}$  atom of threonine phosphate until the N–H group of phenylalanine (in total 20 atoms represented as balls in Figure 5). Because of the high computational cost windows, only every 20° (except for the region around the maximum of the mean reaction force) was considered, and only 15 ps per window could be simulated. Extending the simulation time to 25 ps for one starting structure did not alter the results considerably, and even longer simulations were not feasible considering the number of windows. The restraining force constant was doubled for simulations around the minimum and maximum of the mean reaction force to minimize the deviation from the restraint value of the reaction coordinate. The QM atoms were treated with the HF/3-21G method, and the link atom method was used for the covalent QM–MM interactions. The chosen QM method is accurate enough to describe the isomerization reaction as evidenced by a detailed study of Kang et al., which shows that the inclusion of electron correlation led to minor changes in the energetics of this reaction in the gas phase and in combination with continuum models.<sup>37</sup>

For the reaction in solution, three simulations with different starting structures were considered per value of the reaction coordinate. In the enzyme, the number of starting structures, where only  $\zeta$  was restraint, was increased to five to account for the heterogeneous nature of the environment provided by the enzyme.

**The Mean Reaction Force (MRF).** To elucidate the mechanistic features that give rise to the catalytic power of Pin1, a complete characterization of the reaction mechanism during the isomerization process is needed. We have made use of the mean reaction Force (MRF), which has proven to unveil valuable mechanistic insights in catalysis at interfaces.<sup>38</sup> It is defined as the negative derivative of the free energy along the reaction path:

$$\langle F(\xi) \rangle = -\frac{dG}{d\xi} \quad (1)$$

Because of its derivation from the free energy along a reaction path, it includes, within a correct description, the influence of the environment on reaction mechanisms, which is crucial in enzyme catalysis. In analogy to the reaction force<sup>39</sup> and as shown previously,<sup>38</sup> it also provides direct access to the characterization of different processes taking place along the path. The minimum and maximum of the mean reaction force divide the reaction path into three regions (see Figure 2): the

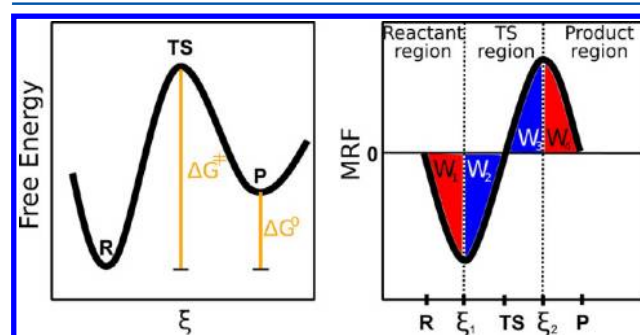


**Figure 2.** Schematic representation of the mean reaction force and free energy profile for an elementary step.

reactant, transition state, and product region. As shown in various previous studies,<sup>40–44</sup> the reactant and product regions involve mostly structural rearrangements of the atoms to reach the transition state from either the reactant or the product. The transition state region encompasses most changes in the electron configuration required to make or break chemical bonds.

With these regions at hand, the activation energy  $\Delta G^\ddagger$  from the reactant can be separated in terms of two contributions  $\Delta G^\ddagger = [G(\xi_{\text{TS}}) - G(\xi_{\text{R}})] = W_1 + W_2$ . The structural  $W_1$  and electronic  $W_2$  contributions (color coded in Figure 2) can be obtained as

$$W_1 = -\int_{\xi_{\text{R}}}^{\xi_{\text{TS}}} \langle F(\xi) \rangle d\xi > 0 \quad W_2 = -\int_{\xi_{\text{TS}}}^{\xi_{\text{P}}} \langle F(\xi) \rangle d\xi > 0 \quad (2)$$

Accordingly, the deactivation from the transition state to the product has an electronic  $W_3$  and structural  $W_4$  part:

$$W_3 = -\int_{\xi_{\text{TS}}}^{\xi_{\text{P}}} \langle F(\xi) \rangle d\xi < 0 \quad W_4 = -\int_{\xi_{\text{R}}}^{\xi_{\text{TS}}} \langle F(\xi) \rangle d\xi < 0 \quad (3)$$

With these contributions, the reaction energy can be expressed as follows:  $\Delta G^\circ = W_1 + W_2 + W_3 + W_4$ .

To obtain the MRF at each value along the reaction coordinate, the Umbrella Integration method of Kästner et al.<sup>45–47</sup> has been employed. The average value of  $\zeta$  was calculated from all simulations that differ in their starting structures. For the error bars in Figures 3 and 4, the standard deviation of the average between the different simulations was added to the average prior to the calculation of the MRF (upper limit) or subtracted (lower limit) representing the 66% confidence interval. The standard deviation of  $\zeta$  required for the calculation of the MRF with Kästner method's was taken as the average over the simulations with different starting structures. Finally, the free energy profile along the reaction



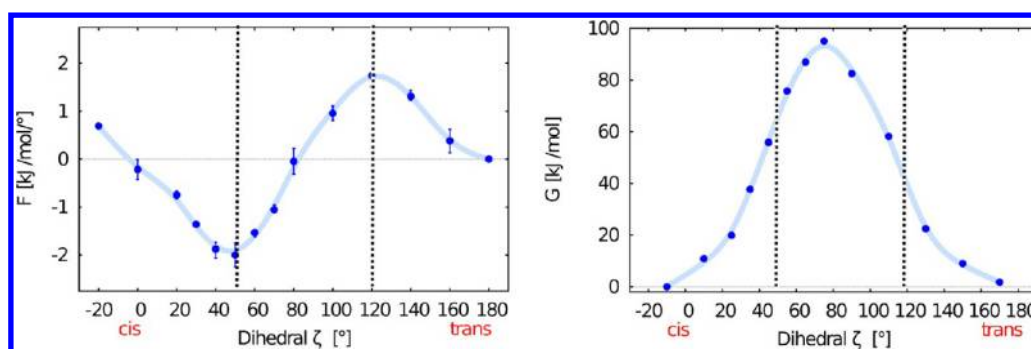


**Figure 3.** Mean reaction force and free energy profile for the cis–trans isomerization of Ace-Gly-pThr-Pro-Phe-Gln-Nme peptide in anticlockwise direction in aqueous solution.

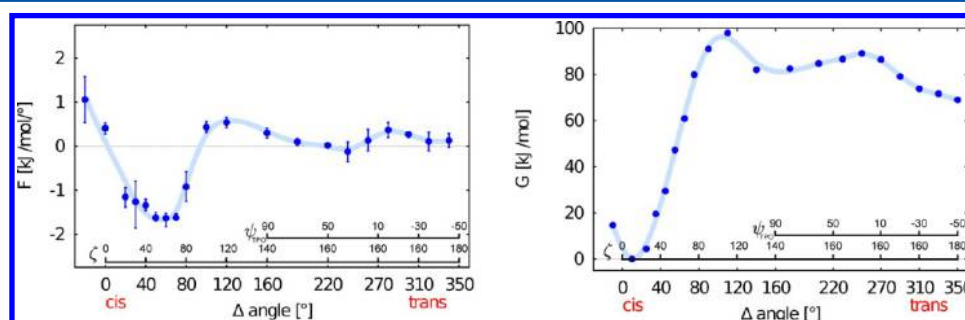


**Figure 4.** Mean reaction force (MRF) and free energy profile for the cis–trans isomerization of Ace-Gly-pThr-Pro-Phe-Gln-Nme peptide in anticlockwise direction in Pin1. The abscissa represents the reaction coordinate as the overall angle of rotation. It only equals  $\zeta$  until  $140^\circ$  and then a combination of  $\zeta$  and  $\psi_{\text{Thr}}$  values.

coordinate was obtained by numerical integration of the MRF applying the Simpson rule.

For the reaction in the enzyme where two reaction coordinates were needed, the mean reaction force was obtained within the linear approximation for each coordinate and the free energy by integration over one and then the other coordinate.

## RESULTS AND DISCUSSION

To discern the origin of the catalytic effect and to compare to the reaction mechanism in the enzyme, the cis–trans isomerization was first studied in aqueous solution. Therefore, the peptide bond preceding the proline residue in the sequence Ace-Gly-pThr-Pro-Phe-Gln-Nme was rotated in water in restraint QM/MM molecular dynamics simulations.

**Isomerization in Aqueous Solution.** The peptide was isolated from the enzyme crystal structure (PDB ID 2Q5A) and equilibrated in aqueous solution for 5 ns (for details, see Methods). The isomerization reaction was followed by restraining consecutively the angle  $\zeta$  (see Figure 1) in  $10^\circ$  steps in anticlockwise rotation (positive values) until the trans configuration ( $\zeta = 180^\circ$ ) was reached. A rotation in the other direction was less favorable in solution and in the enzyme and therefore not considered (see the Supporting Information). From each window of the simulations described above, three structures of the last 4 ns were employed for subsequent QM/MM molecular dynamics simulations (for details, see Methods).

The mean reaction force (MRF) and the free energy profile along the reaction coordinate  $\zeta$  are shown in Figure 3. The cis configuration presents a minimum at  $\zeta \leq 0^\circ$  where the MRF is zero. The MRF crosses zero again at the transition state ( $\zeta = 180^\circ$ ) and reaches the product represented by the trans isomer

at  $180^\circ$ . Its minimum, which describes the point of overtaking electronic rearrangements along the reaction coordinate, is reached at  $\approx 50^\circ$  and the maximum describing the almost completed electronic reorganization and the onset of structural relaxation at  $120^\circ$ .

The free energy profile exhibits an activation barrier to reach the transition state from the cis isomer  $\Delta G_{\text{c} \rightarrow \text{t}}^\ddagger$  of  $95 \pm 10$  kJ/mol (error is estimated as one-half the difference from the free energy obtained using the MRF including the error bars). This value compares well with the value of 105 kJ/mol of Yonezawa et al. who studied the cis–trans isomerization of Ace-Pro-Nme in explicit water with QM/MM simulations<sup>48</sup> and the experimental value of 84.1 kJ/mol for the Ala-Ala-Thr-( $\text{PO}_3^{2-}$ )-Pro-Phe-NH-Np of Schutkowski et al.<sup>13</sup> The cis–trans free energy difference  $\Delta G_{\text{c} \rightarrow \text{t}}^0$  of 2 kJ/mol represents almost isoenergetic cis and trans conformers considering the integration errors and the error bars. According to Schutkowski et al.,<sup>13</sup> the content of cis conformer lies at 6.4%, resulting in an experimental value for  $\Delta G_{\text{c} \rightarrow \text{t}}^0$  at 298 K of  $-6.7$  kJ/mol.

As shown in a previous study by us,<sup>38</sup> the separation of the reaction in different regions derived from the mean reaction force allows one to assign structural and electronic contributions to the free energy barrier (see Methods). The activation of the cis isomer is dominated by the structural contribution  $W_1 = 65$  kJ/mol and a small electronic part of  $W_2 = 30$  kJ/mol. Once the transition state is reached, the system relaxes with an electronic contribution of  $W_3 = -55$  kJ/mol and a structural component of  $W_4 = -38$  kJ/mol.

To validate the separation of the reaction mechanism in electronic and structural changes by the mean reaction force, an independent descriptor of electronic activity was also considered. During the isomerization, the nitrogen atom of the peptide bond turns from a  $\text{sp}^2$ - to a  $\text{sp}^3$ -hybridization at the

transition state that locates the free electron pair on the nitrogen atom. This is accompanied by a change in bond character of the peptide bond from pseudo double to single bond at the transition state and should be reflected in an increase of the peptide bond length. Indeed, as shown in the Supporting Information, the largest changes in the bond length are observed between  $\zeta = 50^\circ$  and  $\zeta = 120^\circ$ , confirming the separation in structural and electronic contributions provided by the minimum and the maximum of the MRF.

Yonezawa et al. reported that the isomerization in aqueous solution is catalyzed by an intramolecular hydrogen bond between the amino hydrogen atom of the residue following proline and the nitrogen atom in the peptide bond. This interaction stabilizes the free electron pair on the nitrogen atom at the transition state and should affect mostly the electronic contribution identified by the MRF. In our simulations, this hydrogen bond, which was present in the starting structure, was preserved during the whole rotation from the cis isomer until  $\zeta = 100^\circ$  in agreement with their results. After the transition state, however, the peptide adopted an extended configuration, and the average distance between these two atoms increased. This indicates the loss of the intramolecular catalysis after the transition state. Indeed, the electronic contribution, which is the one most affected by the hydrogen bond, is larger for the reverse reaction starting from the trans isomer ( $|W_3| > W_2$ ). Therefore, the mean reaction force correctly identifies the catalytic effect of the intramolecular hydrogen bond decreasing the electronic contribution by  $\approx 20$  kJ/mol. This catalytic active intramolecular hydrogen bond in the isomerization reaction in solution was also proposed in an experimental study by Cox et al.<sup>49</sup> and in the enzymatic rotamase catalysis of FK506 binding protein by Fischer et al.<sup>34</sup>

**Isomerization in Pin1.** In a second step, the cis–trans isomerization of the same Ace-Gly-pThr-Pro-Phe-Gln-Nme peptide was also studied in the enzyme.

As in solution, the preferred direction of rotation is in anticlockwise direction (toward positive values). Along this direction of rotation, which is noted with the arrow in Figure 1, the carbonyl oxygen atom interacts with the enzyme residues Cys-113 and Ser-154. In the unfavorable opposite direction, the carbonyl group has to rotate inside of the IVa-turn formed by the peptide, disrupting the intramolecular hydrogen bond, found to catalyze the reaction in solution.

A representative reactant structure at  $\zeta = 0^\circ$  is shown in Figure 5 together with a structure at  $90^\circ$  representing the transition state. As can be seen from their comparison, only the peptide residues preceding proline rotate (left part of the peptide in Figure 5), whereas the other residues are kept fixed through hydrogen bonds to the enzyme backbone described in the Introduction and shown in Figure 1.

To ensure enough sampling of possible peptide and enzyme conformations, five starting structures from the last 4 ns of the MM simulations were used as input for QM/MM molecular dynamics simulations for each window, yielding a total simulation time of more than 600 ps (for simulations restraining only  $\zeta$ ).

The obtained MRF profile until the transition state shown in Figure 4 can now be compared to the reaction in solution to elucidate possible changes in the reaction mechanism. The enzyme shifts the minimum of the cis isomer to  $\zeta$  values larger than zero and toward the transition state, leaving the value of the MRF minimum unaffected at  $50^\circ$ . The transition state is also shifted to  $90^\circ$  with respect to the value in solution of  $80^\circ$ .

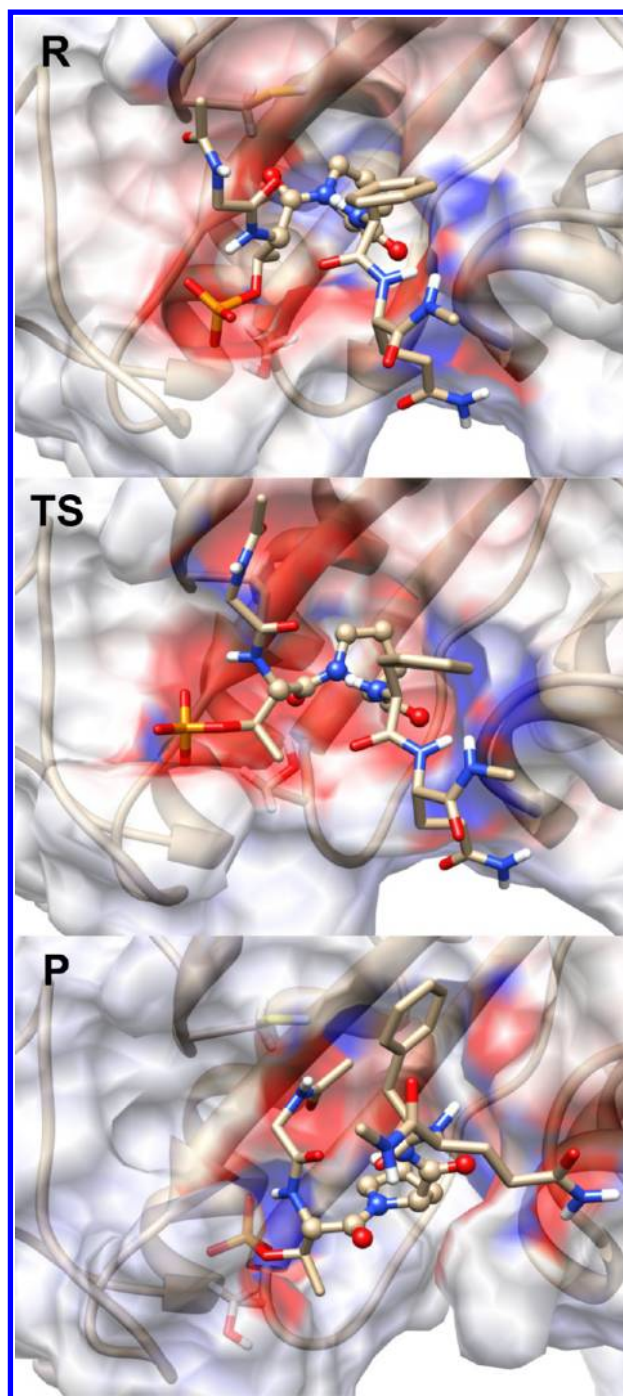


**Figure 5.** Representative snapshots of the cis isomer, transition state ( $\zeta = 90^\circ$ ), and the product ( $\zeta = 180^\circ, \psi_{\text{pThr}} = -50^\circ$ ). Atoms representing the QM region are presented as spheres. The surface accessible surface is colored according to the electrostatic potential (blue = +256.71 mV; red = -256.71 mV) calculated with the APBS software and taking only the peptide and enzyme atoms into account.

The free energy barrier to reach the transition state from the cis isomer  $\Delta G_{\text{c-t}}^\ddagger$  equals  $98 \pm 10$  kJ/mol, matching the barrier in solution (error is estimated as one-half the difference from the free energy obtained using the MRF including the error bars).

In analogy to the isomerization in solution, contributions to the activation barrier originated from electronic activity (changes in the electron configuration) or structural rearrangements have been identified through the MRF. In the enzyme,

the value for  $W_1$  that represents the structural contribution is 38 kJ/mol, and the electronic part  $W_2$  amounts to 60 kJ/mol. The smaller value of  $W_1$  with respect to the solution reaction indicates that the enzyme reduces the energy needed to fulfill the structural rearrangements to reach the transition state, which is in line with the shift of the minimum of the cis isomer. This reduction can be understood as either the electrostatic preorganization concept<sup>50</sup> of the enzyme that reduces the reorganization energy associated with the environmental response polarized by the changed solute charges or the destabilization of the reactant in the enzyme with respect to solution as was already observed by Fischer et al. for the rotamase catalysis of the FK506 binding protein.<sup>34</sup>

The reduction in the energy required for the structural rearrangements, however, is counterbalanced by  $W_2$ , the energy that involves the reorganization of the electrons' configuration in the enzyme. To discern possible effects of the environment on this reorganization, the electrostatic potential, arising from the enzyme and the peptide, was calculated for representative structures of the cis isomer and the transition state ( $\zeta = 90^\circ$ ) with the APBS software<sup>51</sup> and mapped into the solvent accessible surface of the enzyme as shown in Figure 5 (for details of the calculation, see the Supporting Information). Throughout the isomerization reaction, the carbonyl group of the threonine residue, which is part of the rotating peptide bond, is surrounded by a negatively charged environment. A negative environment, in principle, should favor the rotation due to a reduction of the double bond character of the peptide bond.<sup>21,52</sup> To track the origin of the negative charge, the electrostatic potential was recalculated, but this time the peptide undergoing the isomerization together with the phosphate group of the threonine residue was not included, resulting in a neutral to positive environment (from the basic residue triad Lys-63, Arg-68, and Arg-69). Therefore, the negative environment originates from the peptide itself and not the enzyme and should in principle also be present for the isomerization in solution, although slightly diminished due to the larger dielectric constant of the surrounding water molecules.

Because global electrostatic influences seem not to be responsible for the increased energy of the reorganization in the electron configuration, direct atom–atom interactions to the carbonyl group of the rotating peptide bond were analyzed. As mentioned in the Introduction and shown in Figure 1, residues Cys-113 and Ser-154 might be involved in direct interactions to the peptide during the isomerization. In fact, for angles smaller than  $50^\circ$ , the carbonyl oxygen atom is loosely bound through a weak hydrogen bond to Cys-113 described by rather small atomic charges of the sulfur and hydrogen atom. This weak interaction might explain the reduced structural contribution to the activation free energy barrier in the enzyme. After the minimum of the MRF, however, the carbonyl oxygen atom interacts with Ser-154 through a strong hydrogen bond, because the hydroxyl group possesses larger atomic charges. This strong hydrogen bond, in contrast to the negative electrostatic potential, would stabilize a negatively charged carbonyl oxygen atom and increase the double bond character of the rotating peptide bond. The increased double bond character impedes the rotation of the bond and the electronic rearrangements necessary to reach the transition state. Therefore, this increased double bond character of the rotating bond through stabilization by strong hydrogen bonds throughout the second region of the MRF explains the larger

energy necessary for the electronic reorganization of the system. It also counterbalances the intramolecular catalysis on the nitrogen atom identified in solution.

Rotating the peptide bond further from the transition state results in unfavorable interactions between its rotating part (left part of the peptide in Figure 1) and the enzyme. These unfavorable interactions are reflected in the MRF when only  $\zeta$  is used as reaction coordinate for the whole isomerization as shown in the Supporting Information. To avoid this interaction that starts at  $\zeta = 140^\circ$ , a second reaction coordinate represented by the  $\psi_{\text{Thr}}$  angle of threonine phosphate residue was considered (see Figure 1). This relaxation pathway to reach the trans isomer after the transition state was already proposed in the work of Velazquez et al.,<sup>36</sup> who applied accelerated molecular dynamics to obtain a free energy map of this angle together with  $\omega$  angle of the peptide bond. We chose values of  $\zeta$  and  $\psi_{\text{Thr}}$  to match the minimum energy path of their proposed free energy map (see Methods).

The reaction coordinate named “angle” in Figure 4 combines in the first part ( $0^\circ \leq \text{angle} \leq 140^\circ$ ) only the rotation of the dihedral angle  $\zeta$  and afterward ( $\text{angle} \geq 140^\circ$ ) a combination of the change in this dihedral angle and the mentioned  $\psi_{\text{Thr}}$  backbone angle that reaches a negative value of  $-50^\circ$  (resulting in values for “angle” larger than  $180^\circ$ ). As can be seen from the MRF profile in Figure 4, the addition of the second angle at  $140^\circ$  leads to values of the MRF around zero and, therefore, avoids the unfavorable interaction with the enzyme. The product is reached at  $\zeta = 180^\circ$  and  $\psi_{\text{Thr}} = -50^\circ$ , which corresponds to the trans isomer with the  $\psi_{\text{Thr}}$  angle in the  $\alpha_{\text{R}}$  region of the Ramachandran plot (see Figure 5, bottom) and matches the minimum obtained by Velazquez et al.<sup>36</sup>

Therefore, in comparison to the reaction in solution, the largest effect of the enzyme is observed in the free energy profile after the transition state toward the trans isomer. If the trans isomer would bind with a  $\psi_{\text{Thr}}$  angle above  $100^\circ$ , which corresponds to the  $\beta$ -region in the Ramachandran plot, the free energy profile derived from the MRF shown in the Supporting Information would predict a steeply decreasing free energy until  $140^\circ$ , a shallow minimum, before reaching the barrier of less than 10 kJ/mol to pass the transition state to the cis isomer. The affinity of Pin1 to this conformer, however, can be assumed to be very small due to the unfavorable interactions discussed above.

It seems much more likely that Pin1 binds the trans conformer in the relaxed form with a  $\psi_{\text{Thr}} = -50^\circ$ , corresponding to the  $\alpha_{\text{R}}$ -region of the Ramachandran plot. Indeed, this region was already identified by Velazquez et al.<sup>36</sup> to be more favorable than the  $\beta$  region for the trans isomer in Pin1. From this conformer, first the  $\psi_{\text{Thr}}$  angle has to be rotated to reach positive values crossing the first transition state with an activation energy of  $\approx 20$  kJ/mol. This transition state is governed by steric interactions of the peptide backbone atoms with the proline ring. Together with the rotation of the  $\psi_{\text{Thr}}$  angle toward positive values,  $\zeta$  decreases and a shallow minimum is reached for  $\zeta = 140^\circ$  and  $\psi_{\text{Thr}} = 90^\circ$ . From this point, only  $\zeta$  decreases toward the transition state at  $\zeta = 90^\circ$  with an activation barrier of less than 20 kJ/mol.

The presence of two minima for the trans isomer was also reported by Fischer et al.,<sup>34</sup> who studied the catalytic effect of FKBP on the cis–trans isomerization of the same peptide bond. They could identify two trans minima that differ in the  $\psi_{\text{Thr}}$  angle preceding the proline residue and were separated by a barrier of 23.4 kJ/mol, which is in agreement with our results.



The obtained results for the whole isomerization in the enzyme and solution can be compared to a recent work of Greenwood et al., who measured NMR spectra of the PPIase domain in combination with part of the APP peptide.<sup>53</sup> Applying line-shape analysis and fitting the signals of five proline protons to a four-state model with seven parameters, they reported a value of 54.5 kJ/mol for the barrier from the cis isomer in the enzyme and a trans isomer with a slightly larger binding constant. The reduction of the barrier with respect to the isomerization in solution (84.4 kJ/mol) was 65%.

From our analysis, we can conclude that the enzyme does not affect the total activation barrier of the cis isomer. If the energetics derived from the NMR measurements are correct, the enzymatic catalysis must be related to another effect, which is not accounted for within our methodology. One possible explanation is that the origin of the catalysis is due to conformational changes in the enzyme that drive the reaction, although this hypothesis has been of considerable debate in the literature.<sup>54–56</sup> These conformational changes, however, occur on a time scale of the NMR experiment and are not accessible with QM/MM molecular dynamics simulations. Indeed, one of the conclusions of the authors in the experimental study was that overall exchange time of the isomers matches the time scale observed of conformational changes.

Our results for the isomerization of the trans isomer, however, show that the enzyme catalyzes the reaction by imposing a consecutive rotation of two angles to reach the transition state from the minimum. Conformational changes of the enzyme may be also involved, contributing to the conversion between the two minima. The observed large decrease in the activation barrier from the trans isomer would also explain why no crystal structure of this isomer could be obtained so far.

## CONCLUSIONS

In summary, the mean reaction force was able to identify structural and electronic contributions to activation barriers and reaction free energies for the isomerization reaction in solution and in the enzyme. In solution, an intramolecular hydrogen bond to the nitrogen atom of the proline ring reduces the energy required for the reorganization of the electron configuration from the cis isomer. The obtained activation barrier improves a recently reported one in a computational study and is closer to the experimental value.

The enzyme does not change the activation barrier from the cis isomer with respect to solution. The separation of the activation barrier by the MRF, however, assigns a reduced structural contribution. This reduction is counterbalanced by a larger electronic part that originates from peptide–enzyme hydrogen bonds, which increase the double bond character of the rotating peptide bond.

The largest influence of the enzyme is observed in the activation of the trans isomer. The presence of the enzyme induces a rotation of the  $\psi_{\text{Thr}}$  angle in the preceding threonine phosphate residue to avoid unfavorable interactions with the rotating part of the peptide. Consideration of this second reaction coordinate results in two stable trans isomers, which can be converted into each other through a small barrier of  $\approx 20$  kJ/mol. From the less stable one, the energy required to reach the transition state amounts to less than 20 kJ/mol, indicating that the isomerization reaction of the trans conformer should be achievable at room temperature in the presence of the enzyme.

All of these results obtained from the mean reaction force, therefore, provide new insights in the mechanism by which Pin1 catalyzes the isomerization reaction.

## ASSOCIATED CONTENT

### Supporting Information

Figure S1 displays the mean reaction force in both directions of rotation in the two different environments (anticlockwise and clockwise). The bond distance of the rotating bond is shown as a function of the reaction coordinate to validate the separation of the contributions provided by the MRF in Figure S2, and relevant distances between enzyme residues participating in the reaction mechanism and the peptide are shown in Figure S3. Finally, a list with the parameters for the electrostatic calculations with the APBS software is available.

This material is available free of charge via the Internet at <http://pubs.acs.org>.

## AUTHOR INFORMATION

### Corresponding Author

\*E-mail: [evohringer@udec.cl](mailto:evohringer@udec.cl).

### Notes

The authors declare no competing financial interest.

## ACKNOWLEDGMENTS

E.V.-M. thanks Proyecto FONDECYT 3110018 for financial support, and A.T.-L. is thankful for support provided by Proyecto FONDECYT 1090460. F.D. acknowledges support from the U.S. Department of State and the Comisión Nacional de Investigación Científica y Tecnológica (CONICYT) in Chile for a Fulbright-CONICYT visiting scholar fellowship. F.D. also thanks CONICYT for a graduate fellowship and Beca Apoyo de Tesis Grant no. 24091124 for financial support.

## REFERENCES

- (1) Stewart, D. E.; Sarkar, A.; Wampler, J. E. *J. Mol. Biol.* **1990**, *214*, 253–260.
- (2) Weiss, M. S.; Jabs, A.; Hilgenfeld, R. *Nat. Struct. Biol.* **1998**, *5*, 676.
- (3) Levitt, M. *J. Mol. Biol.* **1981**, *145*, 251–263.
- (4) Kieffhaber, T.; Grunert, H. P.; Hahn, U.; Schmid, F. X. *Biochemistry* **1990**, *29*, 6475–6480.
- (5) Sarkar, P.; Reichman, C.; Saleh, T.; Birge, R. B.; Kalodimos, C. G. *Mol. Cell* **2007**, *25*, 413–426.
- (6) Lummis, S. C. R.; Beene, D. L.; Lee, L. W.; Lester, H. A.; Broadhurst, R. W.; Dougherty, D. A. *Nature* **2005**, *438*, 248–252.
- (7) Wu, X.; Wilcox, C.; Devasahayam, G.; Hackett, R.; Arevalo-Rodriguez, M.; Cardenas, M.; Heitman, J.; Hanes, S. *EMBO J.* **2000**, *19*, 3727–3738.
- (8) Nelson, C. J.; Santos-Rosa, H.; Kouzarides, T. *Cell* **2006**, *126*, 905–916.
- (9) Ryo, A.; Liou, Y.; Wulf, G.; Nakamura, M.; Lee, S.; Lu, K. *Mol. Cell. Biol.* **2002**, *22*, 5281–5295.
- (10) Suizu, F.; Ryo, A.; Wulf, G.; Lim, J.; Lu, K. *Mol. Cell. Biol.* **2006**, *26*, 1463–1479.
- (11) Lu, K. P.; Finn, G.; Lee, T. H.; Nicholson, L. K. *Nat. Chem. Biol.* **2007**, *3*, 619–629.
- (12) Butterfield, D.; Abdul, H. M.; Opii, W.; Newman, S. F.; Joshi, G.; Ansari, M. A.; Sultana, R. *J. Neurochem.* **2006**, *98*, 1697–1706.
- (13) Schutkowski, M.; Bernhardt, A.; Zhou, X. Z.; Shen, M.; Reimer, U.; Rahfeld, J.-U.; Lu, K. P.; Fischer, G. *Biochemistry* **1998**, *37*, 5566–5575.
- (14) Hamelberg, D.; Shen, T.; McCammon, J. A. *J. Am. Chem. Soc.* **2005**, *127*, 1969–1974.
- (15) Cohen, P. *Trends Biochem. Sci.* **2000**, *25*, 596–601.

- (16) Lu, K.; Hanes, S.; Hunter, T. *Nature* **1996**, *380*, 544–547.
- (17) Yaffe, M. *Science* **1997**, *278*, 1957–1960.
- (18) Zhou, X.; Kops, O.; Werner, A.; Lu, P.; Shen, M.; Stoller, G.; Kullertz, G.; Stark, M.; Fischer, G.; Lu, K. P. *Mol. Cell* **2000**, *6*, 873–883.
- (19) Ranganathan, R.; Lu, K. P.; Hunter, T.; Noel, J. P. *Cell* **1997**, *89*, 875–886.
- (20) Schroeder, O. E.; Carper, E.; Wind, J. J.; Poutsma, J. L.; Etzkorn, F. A.; Poutsma, J. C. *J. Phys. Chem. A* **2006**, *110*, 6522–6530.
- (21) Behrsin, C.; Bailey, M.; Bateman, K.; Hamilton, K.; Wahl, L.; Brandl, C.; Shilton, B.; Litchfield, D. *J. Mol. Biol.* **2007**, *365*, 1143–1162.
- (22) Bailey, M.; Shilton, B.; Brandl, C.; Litchfield, D. *Biochemistry* **2008**, *47*, 11481.
- (23) Hess, B.; Kutzner, C.; van der Spoel, D.; Lindahl, E. *J. Chem. Theory Comput.* **2008**, *4*, 435–447.
- (24) Bussi, G.; Donadio, D.; Parrinello, M. *J. Chem. Phys.* **2007**, *126*, 014101.
- (25) Berendsen, H. J. C.; Postma, J. P. M.; van Gunsteren, W. F.; Nola, A. D.; Haak, J. R. *J. Chem. Phys.* **1984**, *81*, 3684–3690.
- (26) Hess, B.; Bekker, H.; Berendsen, H.; Fraaije, J. J. *Comput. Chem.* **1997**, *18*, 1463–1472.
- (27) Frisch, M. J.; Trucks, G. W.; Schlegel, H. B.; Scuseria, G. E.; Robb, M. A.; Cheeseman, J. R.; Montgomery, J.; Vreven, T.; Kudin, K. N.; Burant, J. C.; et al. *Gaussian 03*, revision D.02; Gaussian, Inc.: Wallingford, CT, 2004.
- (28) Zhang, Y.; Daum, S.; Wildemann, D.; Zhou, X. Z.; Verdecia, M. A.; Bowman, M. E.; Lücke, C.; Hunter, T.; Lu, K.-P.; Fischer, G.; et al. *ACS Chem. Biol.* **2007**, *2*, 320–328.
- (29) Hornak, V.; Abel, R.; Okur, A.; Strockbine, B.; Roitberg, A.; Simmerling, C. *Proteins: Struct., Funct., Bioinf.* **2006**, *65*, 712–725.
- (30) Craft, J. W., Jr; Legge, G. B. *J. Biomol. NMR* **2005**, *33*, 15–24.
- (31) Bayer, E.; Goettsch, S.; Mueller, J. W.; Griewel, B.; Guiberman, E.; Mayr, L. M.; Bayer, P. *J. Biol. Chem.* **2003**, *278*, 26183–26193.
- (32) Jacobs, D. M.; Saxena, K.; Vogtherr, M.; Bernado, P.; Pons, M.; Fiebig, K. M. *J. Biol. Chem.* **2003**, *278*, 26174–26182.
- (33) Hermans, J.; Berendsen, H. J. C.; Van Gunsteren, W. F.; Postma, J. P. M. *Biopolymers* **1984**, *23*, 1513–1518.
- (34) Fischer, S.; Michnick, S.; Karplus, M. *Biochemistry* **1993**, *32*, 13830–13837.
- (35) Fischer, S.; Dunbrack, R. L.; Karplus, M. *J. Am. Chem. Soc.* **1994**, *116*, 11931–11937.
- (36) Velazquez, H. A.; Hamelberg, D. *Biochemistry* **2011**, *50*, 9605–9615.
- (37) Jhon, J.; Kang, Y. *J. Phys. Chem. A* **1999**, *103*, 5436–5439.
- (38) Vöhringer-Martinez, E.; Toro-Labbé, A. *J. Chem. Phys.* **2011**, *135*, 64505.
- (39) Toro-Labbé, A. *J. Phys. Chem. A* **1999**, *103*, 4398–4403.
- (40) Herrera, B.; Toro-Labbé, A. *J. Chem. Phys.* **2004**, *121*, 7096–7102.
- (41) Rincón, E.; Jaque, P.; Toro-Labbé, A. *J. Phys. Chem. A* **2006**, *110*, 9478–9485.
- (42) Burda, J. V.; Toro-Labbé, A.; Gutiérrez-Oliva, S.; Murray, J. S.; Politzer, P. *J. Phys. Chem. A* **2007**, *111*, 2455–2457.
- (43) Vöhringer-Martinez, E.; Toro-Labbé, A. *J. Comput. Chem.* **2010**, *31*, 2642–2649.
- (44) Duarte, F.; Vöhringer-Martinez, E.; Toro-Labbé, A. *J. Phys. Chem. Chem. Phys.* **2011**, *13*, 7773–7782.
- (45) Kästner, J.; Thiel, W. *J. Chem. Phys.* **2005**, *123*, 144104.
- (46) Kästner, J.; Thiel, W. *J. Chem. Phys.* **2006**, *124*, 234106.
- (47) Kästner, J. *Wiley Interdiscip. Rev.: Comput. Mol. Sci.* **2011**, *1*, 932–942.
- (48) Yonezawa, Y.; Nakata, K.; Sakakura, K.; Takada, T.; Nakamura, H. *J. Am. Chem. Soc.* **2009**, *131*, 4535–4540.
- (49) Cox, C.; Lectka, T. *J. Am. Chem. Soc.* **1998**, *120*, 10660–10668.
- (50) Warshel, A. *Proc. Natl. Acad. Sci. U.S.A.* **1978**, *52*, 5250–5254.
- (51) Holst, M.; McCammon, J. *Proc. Natl. Acad. Sci. U.S.A.* **2001**, *98*, 10037–10041.
- (52) Fischer, G. *Chem. Soc. Rev.* **2000**, *29*, 119–127.
- (53) Greenwood, A. I.; Rogals, M. J.; De, S.; Lu, K.-P.; Kovrigina, E. L.; Nicholson, L. K. *J. Biomol. NMR* **2011**, *51*, 21–34.
- (54) Labeikovsky, W.; Eisenmesser, E. Z.; Bosco, D. A.; Kern, D. *J. Mol. Biol.* **2007**, *367*, 1370–1381.
- (55) Pislakov, A. V.; Cao, J.; Kamerlin, S. C. L.; Warshel, A. *Proc. Natl. Acad. Sci. U.S.A.* **2009**, *106*, 17359–17364.
- (56) Johansson, D. G. A.; Wallin, G.; Sandberg, A.; Macao, B.; Åqvist, J.; Härd, T. *J. Am. Chem. Soc.* **2012**, *131*, 9475–9477.